Evolution of the WC grain shape in WC-Co alloys during sintering: Cumulated effect of the Cr addition and of the C content

Aurélie Delanoë, Sabine Lay

Evolution of the WC grain shape in WC–Co alloys during sintering: Cumulated effect of the Cr addition and of the C content

Aurélie Delanoë, Sabine Lay *

Science et Ingénierie des Matériaux et Procédés, INPGrenoble-CNRS-UJF, BP75, 38402 St. Martin-d'Hères Cedex, France

The evolution of the WC grain shape in Cr doped WC–Co alloys is studied at several stages of the sintering treatment. The common shape of WC is a prism based on a truncated triangle. The habit planes are two prismatic facets and the basal plane. In this work, the WC grain morphology is quantified using transmission electron microscopy at several temperatures. Two shape factors are used to measure the anisotropy between the two prismatic facets and between the prismatic and basal facets. The cumulated effect of the Cr addition and C content is studied. The Cr addition increases the anisotropy between prismatic facets in the W rich alloy. A significant increase of the elongation factor is recorded in the C rich alloy while the effect is more limited in the W rich alloy. The results are discussed as a function of the factors influencing the grain shape: grain growth and difference in energy between the facets.

1. Introduction

WC–Co cemented carbides are usually obtained by liquid phase sintering of a mixture of WC and Co powders. They consist in faceted WC grains embedded in a Co rich binder. The shape of the WC grains is a truncated triangular prism terminated by two kinds of {10–10} prismatic facets and the (0001) basal plane [1]. Submicronic or even finer WC powders are used to improve the mechanical properties of the alloys, which leads to enhanced grain growth during the sintering process [2,3]. Grain growth inhibitors like VC, TaC or Cr_3C_2 are added in order to limit this effect [4].

The WC grain shape [2,5,6], especially the truncation of the triangular prism [7], is reported to depend on the C potential of the alloy. The Co content is observed to change the elongation of the WC grains [8]. Additions of transition metal carbides also influence the grain morphology. Cr_3C_2 additions generate partly rounded WC grains [9] while VC would induce sharp triangular grains [10]. In TiC doped WC–Ni alloys, the shape equixiality of WC grains was shown to be influenced by the Ni amount and the Ti concentration [11]. The typical shape of the WC grains denotes differences between the energies of the three types of facets. The morphology variations observed in various alloys underline the composition effect on the anisotropy of the facets energies. Such effects are not quantified because the facet energies are difficult to measure and only the mean value of interface energy was estimated at 0.5 Jm^{-2} [12]. An evaluation of the composition effect on the interface energies was carried out using a theoretical approach [13,14]. The interface energy ratios of the facets can also be deduced experimentally from the grain shape when the shape is at the equilibrium. A study of the morphology of WC grains in ternary WC–Co alloys containing a C or a W excess was first achieved in [15]. In the present work, the effect of the cumulated effect of the C/W ratio and Cr addition is investigated. The morphology of WC grains is characterised at several stages of the sintering treatment for alloys containing a standard amount of Co. Alloys containing a larger amount of Co and sintered for a longer time were also designed in order to achieve a microstructure close to the equilibrium. Two shape factors are used to measure the anisotropy between prismatic planes and the one between prismatic and basal planes. The results concerning the Cr rich alloys will first be presented. Then the effect of the Cr addition will be determined by comparing the results with those of the ternary alloys.

2. Materials and method

2.1. Alloy preparation

The alloys used in this work are partly the same as those described in [9]. The Co for Cr substitution rate was chosen equal to 5%. The literature data on the constitution of WC–Co–Cr alloys [16,17] indicate that for this value Cr dissolves in the binder. Two compositions with a Co + Cr content close to 13 at% called WC–13Co, Cr, C and WC–13Co, Cr, W were used to study the cumulated effect of C content and Cr addition (Table 1). The alloys are expected to lie in the three phase fields {WC + Co rich binder + C_g} and {WC + Co rich binder + M_6C (M = W, Co, Cr)} at 1450 °C. The C/W ratios are equal to 1.05 and 0.97, respectively. They were

* Corresponding author. Tel.: +33 0 476826628; fax: +33 0 476826744.
E-mail address: sabine.lay@simap.grenoble-inp.fr (S. Lay).

Table 1
Compositions of the alloys

	Composition (at%)					Composition (at%)		
	Co	Cr	C	W		Co	C	W
WC–13Co, Cr, C*	12.4	0.65	44.55	42.4	WC–13Co, C*	13	44.45	42.55
WC–13Co, Cr, W*	12.2	0.6	42.9	44.3	WC–13Co, W*	13	42.8	44.4
WC–34Co, Cr, C (10 h)	32.7	1.8	36.2	29.3	WC–34Co, C (10 h)	34.5	36.2	29.3
WC–34Co, Cr, W (10 h)	32.7	1.8	29.3	36.2	WC–34Co, W (10 h)	34.5	29.3	36.2

The star indicates the composition of the alloy after sintering for 2 h at 1450 °C while the other values correspond to the nominal composition.

prepared from WC, Co and Cr_3C_2 powders with 0.9 μm, 1.5 μm and 3.6 μm in size respectively. Graphite or W powders were added to adjust the C content. The powder mixtures were ball milled for 5 h. The compacts were heated in a graphite furnace for various times and temperatures using the processing conditions described in detail in [5]. The sintering treatment was interrupted in order to study the evolution of the WC grain shape after 1 h at 1200 °C, during the heating stage at 1350 °C and at 1450 °C after 2 h. The melting temperature of the binder was determined to be 1220 °C in WC–13Co, Cr, C and 1330 °C in WC–13Co, Cr, W alloy [18]. The effect of a long liquid phase sintering time was studied using a treatment of 10 h at 1450 °C. A larger Co content with a Co+Cr amount close to 34 at% was chosen in order to reduce the effect of contacts on the grain shape. The Co for Cr substitution rate was also fixed to 5%. In order to control the C loss occurring during the heating stage, two compositions called WC–34Co, Cr, C (10 h) and WC–34Co, Cr, W (10 h) also lying in the three phase fields with C/W ratios equal to 1.2 and 0.8 were selected. These alloys were prepared from WC powders with 0.85 μm as medium size and the holding time at 1200 °C was also longer (12 h) (Table 1).

Results are compared with those of WC–Co alloys free from Cr. Their preparation is described in [5]. Two ternary compositions called WC–13Co, C and WC–13Co, W containing about 13 at% of Co and a C or a W excess were sintered. The C/W ratios are equal to 1.04 and 0.96 respectively. The alloys lie in the three phase fields {WC + Co rich binder + C_g} and {WC + Co rich binder+M_6C (M = W, Co)} respectively, at 1450 °C [19]. Alloys with a larger amount of Co with a C or a W excess called WC–34Co, C (10 h) and WC–34Co, W (10 h) were also elaborated (Table 1).

2.2. Shape factors and experimental procedure

The shape of WC grains is a truncated triangle prism terminated by two kinds of {10–10} prismatic facets and the (0001) basal plane (Fig. 1). Two shape factors were used to quantify the morphology of the grains: the truncation factor measures the anisotropy between the two sets of prismatic facets while the elongation factor measures the anisotropy between the prismatic and basal facets.

2.2.1. The truncation factor r

WC has a hexagonal unit cell (P-6m2) with W atoms at (0,0,0) and C atoms at (1/3, 2/3, 1/2) positions (a = 0.2906 nm and c = 0.2837 nm). WC has no symmetry centre so the {10–10} et {−1010} facets are not equivalent. When WC grains are observed along ⟨0001⟩ their projection is a truncated triangle. $r = \Sigma a_{short} / \Sigma a_{long}$ is the ratio between the length of the two types of facets (Fig. 1).

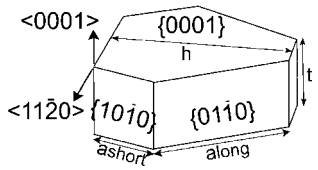

Fig. 1. Morphology of WC grains in WC–Co alloys showing the (0001) basal and {10–10} prismatic facets.

In the assumption of an equilibrium shape the r factor depends on the energy of the two types of facets. The broadest facet is called P^{long} and the shortest P^{short}. The broadest facets are related to the smallest energy γ^{Plong} and the shortest ones to the highest energy γ^{Pshort} (1). A truncation factor equal to 1 corresponds to hexagonal grains and expresses the equality between the interfaces energies. On the contrary, a triangular shape is related to a difference in energy.

$$r = \frac{\frac{2\gamma Plong}{\gamma Pshort} - 1}{\left(2 - \frac{\gamma Plong}{\gamma Pshort}\right)} \quad (1)$$

2.2.2. The elongation factor k

When WC grains are observed along the ⟨11−20⟩ direction their projection is a rectangle. $k = t/h$ is the ratio of the thickness of the prism over the height of the truncated triangle (Fig. 1).

In the assumption of an equilibrium shape, the factor k is related to the γ^{Plong} and γ^{B} energies of the P^{long} facet and of the basal facet called B by Eq. (2) that takes into account the truncation factor [14]:

$$k = \frac{2\gamma B(2r+1)}{3\gamma Plong(r+1)} \quad (2)$$

Transmission electron microscopy (TEM) was used to quantify the grain shape because it permits to precisely orientate the grains along special directions. The thin foils were prepared by mechanical thinning then milled by argon ions. Observations were performed on a 3010 JEOL microscope. The limitation of this technique is to observe areas less than about 1 μm thick while the size of the studied grains is usually larger than 1 μm. The measurement of the r values is valuable whatever the WC grain size because the truncated triangle has the same projection along the [0001] direction whatever the specimen thickness. On the contrary if the middle of the WC grain is not contained in the TEM specimen the height h is underestimated and the k factor is overestimated. In order to avoid this problem only the largest grains with the largest height values were considered. This choice induces that only the k values of the largest grains were retained.

2.2.3. Dispersion of the results and precision of the shape factors

Several TEM thin foils were examined for each alloy. At least 20 grains were studied for the determination of each shape factor. For each alloy it was checked that the grain size range of the grains studied by TEM was roughly the same as the one detected by scanning electron microscopy (SEM) observations. The values obtained far from the mean value were not considered. For the other measurements a mean value × was determined (3) as well as the standard deviation σ to evaluate the scattering of the distribution (4):

$$x = \frac{1}{n}\sum x_i \tag{3}$$

$$\sigma = \sqrt{\frac{1}{n(n-1)}}\sqrt{(x_i - x)^2} \tag{4}$$

where n is the number of measurements.

Due to the limited number of measurements, the Student law was used to determine a reliable interval for the mean value. According to this law there is a probability of 90% that x lie in the interval [x −1.7 $\sigma/\sqrt{}$n x +1.7$\sigma/\sqrt{}$n]. In what follows, the mean values of the factors will be given according to the relation x ± 1.7 $\sigma/\sqrt{}$n.

2.3. Additional characterisation

Further investigations of the alloys sintered at 1200 °C were carried out by energy dispersive X-ray spectroscopy (EDS) in order to study the distribution of Cr. A spot size of about 10 nm was used to study the WC/Co interfaces. The results were quantified using the thickness of the analysed area and the phase density. A mean thickness of 200 nm was chosen since the result is not very sensitive to this parameter. The density was taken equal to 9 gcm^{-3} for the binder, 15 gcm^{-3} for WC and 12 gcm^{-3} for the interface. The interfaces were also imaged by high resolution electron microscopy (HRTEM) using a 4000EX JEOL microscope. For the EDS analyses and HRTEM observations the same parameters as described in [20] were used.

3. Results

3.1. Microstructure of the alloys

The microstructure of the WC–13Co, Cr, C and WC–13Co, Cr, W alloys was quantified by SEM for the sintering treatments at 1450 °C in [9]. Two populations of WC grains were defined: the ones being in the peak of the intercept distributions that are the most numerous and are called the matrix grains and large grains being in the tail of the intercept distributions. It was shown that the addition of Cr in the C rich alloy reduces the peak broadening and the development of the tail but some large grains form in this alloy. In the W rich alloy, the Cr addition has nearly no effect on the matrix grains, while the large grain formation is nearly prevented. The effect of Cr addition was checked in the alloys sintered for 10 h and containing a larger amount of Co. Their microstructure was observed by SEM (Fig. 2). As expected a large amount of M_6C grains was found in WC–34Co, Cr, W (10 h). The microstructure of WC–13Co, Cr, C and WC–13Co, Cr, W sintered at 1350 °C is also shown. At this stage the densification is not achieved and large pores are present. Although the WC starting powder is not exactly the same as in the alloys containing 34 at% of Co the comparison of the images shows that grain growth was limited in WC–34Co, Cr, C (10 h) and very limited in WC–34Co, Cr, W (10 h). The intercept distributions were determined from the measurement of at least 600 intercepts and compared to those obtained in WC–34Co, C (10 h) and WC–34Co, W (10 h). The results for WC–13Co, Cr, C and WC–13Co, Cr, W alloys sintered for 2 h at 1450 °C are also indicated (Fig. 3).

In WC–34Co, C (10 h) matrix grains roughly range between 0.5–3 μm and large ones between 6–17 μm [15]. The addition of Cr significantly modifies the intercept distribution. In WC–34Co, Cr, C (10 h) the peak is narrower, it is shifted towards smaller values and no large grains has developed. The mean intercept value is equal to 0.62 μm while it is equal to 1.8 μm in the Cr free alloy. The microstructure is slightly coarser in WC–13Co, Cr, C sintered for 2 h at 1450 °C. Compared to WC–34Co, Cr, C (10 h), the peak of the matrix grains is shifted towards larger values and large grains are present in the range 2–5 μm.

In WC–34Co, W (10 h) the two sets of grains are also present. The matrix grains range between 0.3–1.2 μm and the largest ones between 1.5–3 μm. The addition of Cr has a limited effect on the grain coarsening in this alloy. In WC–34Co, Cr, W (10 h) the matrix grains are slightly smaller, they range between 0.1–1.0 μm and the largest ones are smaller than about 2 μm. In this alloy the mean intercept value is 0.53 μm while it is equal to 0.7 μm in WC–

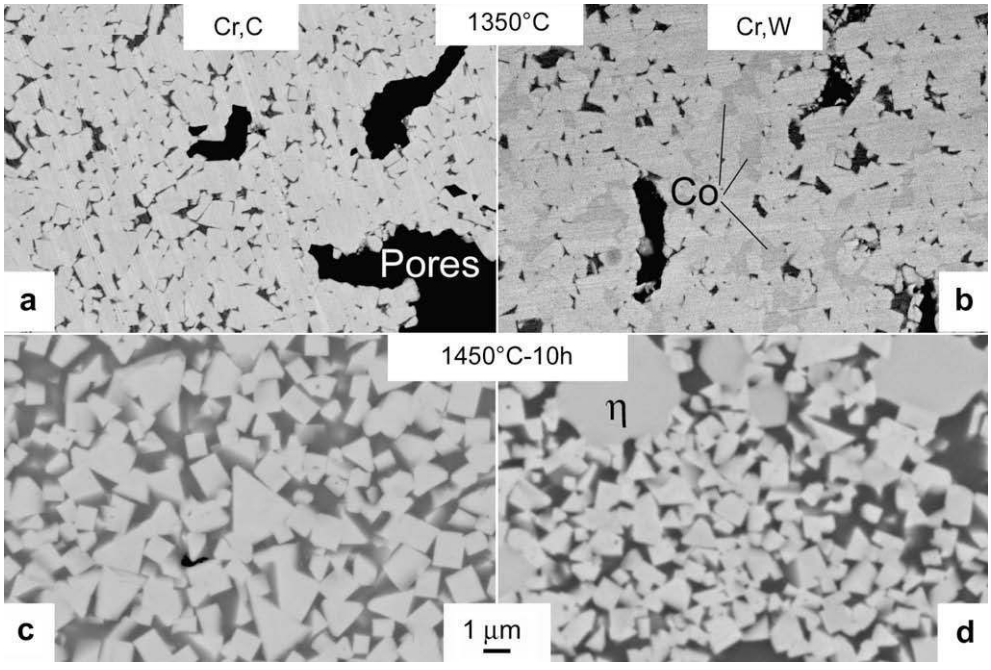

Fig. 2. SEM images of (a,b) WC–13Co, Cr, C and WC–13Co, Cr, W sintered at 1350 °C and (c,d) WC–34Co, Cr, C (10 h) and WC–34Co, Cr, W(10 h) sintered for 10 h at 1450 °C. M_6C grains are referred to as η.

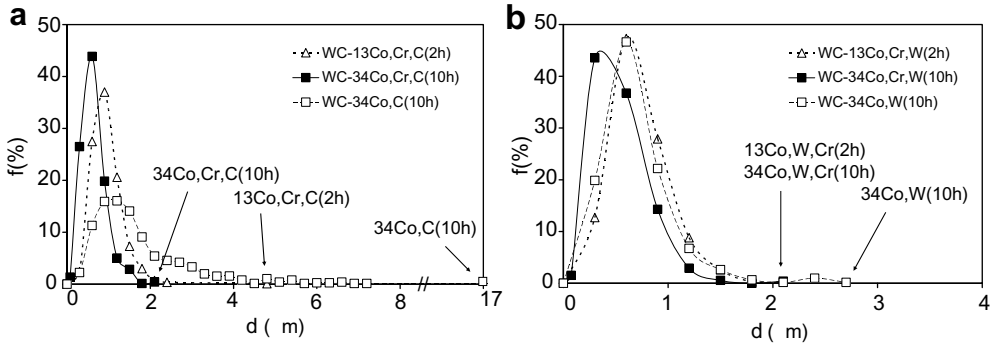

Fig. 3. (a) Comparison of the intercept distributions of the C rich alloys sintered for 2 h and 10 h at 1450 °C. (b) Comparison of the intercept distributions of the W rich alloys sintered for 2 h and 10 h at 1450 °C.

34Co, W (10 h). The intercept distribution of WC–13Co, Cr, W sintered for 2 h is nearly the same as in WC–34Co,W(10 h).

3.2. Study of the WC grain truncation in the Cr doped alloys

After the heating stage at 1200 °C for 1 h WC grains are facetted according to the prismatic and basal facets. The P^{long} prismatic facet is usually smooth while P^{short} is straight or rounded (Fig. 4a, b). The *r* values are given as a function of the size of the WC grains. This latter corresponds to the side of a triangle with a surface equal to that of the observed truncated triangle. The measurements detect a mean value of 0.35 ± 0.06 in WC–Co,Cr,C and a close value of 0.30 ± 0.06 in WC–Co, Cr, W (Table 2). A significant scattering is observed in both alloys (Fig. 5a).

At 1350 °C no evolution is observed in WC–13Co, Cr, C. A mean value of 0.35 ± 0.05 is found in this alloy after liquid formation. In WC,13Co, Cr, W *r* decreases up to 0.21 ± 0.03. The scattering of the distribution is still rather large (Fig. 5b).

After 2 h at 1450 °C, a decrease of the *r* value and of the scattering is recorded in the C rich alloy. In WC–13Co, Cr, C a mean value of 0.26 ± 0.04 is obtained and a nearly unchanged value of 0.19 ± 0.04 is measured in WC–13Co, Cr, W. No difference is

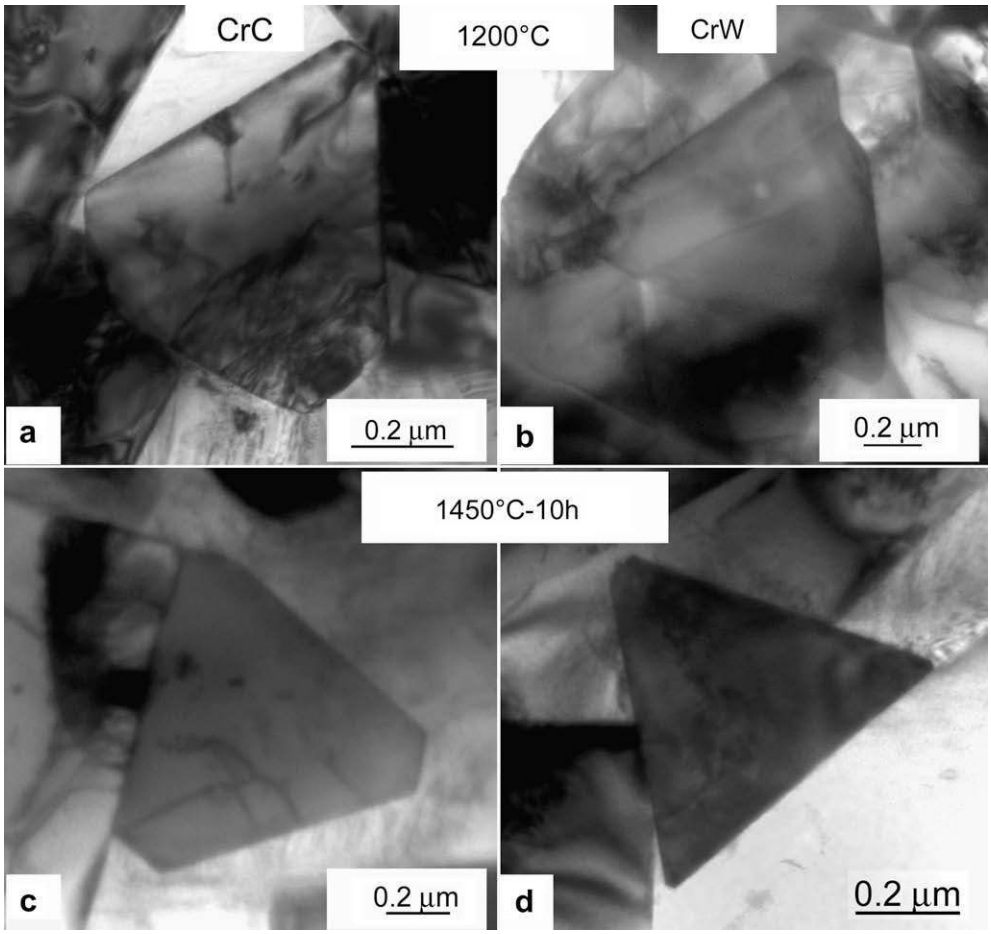

Fig. 4. TEM images of the WC grains viewed along the [0001] direction in the alloys sintered at 1200 °C (a) WC–13Co, Cr, C with *r* = 0.32 and (b) WC–13Co, Cr, W with *r* = 0.31, and in the alloys sintered for 10 h at 1450 °C (c) WC–34Co, C, Cr (10 h) with *r* = 0.18 (d) WC–34Co, W, Cr with *r* = 0.05.

Table 2
Mean truncation values *r*, standard deviation of the distribution σ, number of measurements n and reliable interval values recorded for the Cr doped C rich and W rich alloys

	Truncation factor							
	C rich				W rich			
	r	*σ*	*n*	$1.7\sigma/\sqrt{n}$	*r*	*σ*	*n*	$1.7\ \sigma/\sqrt{n}$
1200 °C–1 h	0.35	0.15	20	0.06	0.30	0.15	20	0.06
1350 °C	0.35	0.15	28	0.05	0.21	0.09	20	0.03
1450 °C–2 h	0.26	0.11	27	0.04	0.19	0.11	26	0.04
1450 °C–10 h (34Co)	0.18	0.07	32	0.02	0.08	0.03	24	0.01

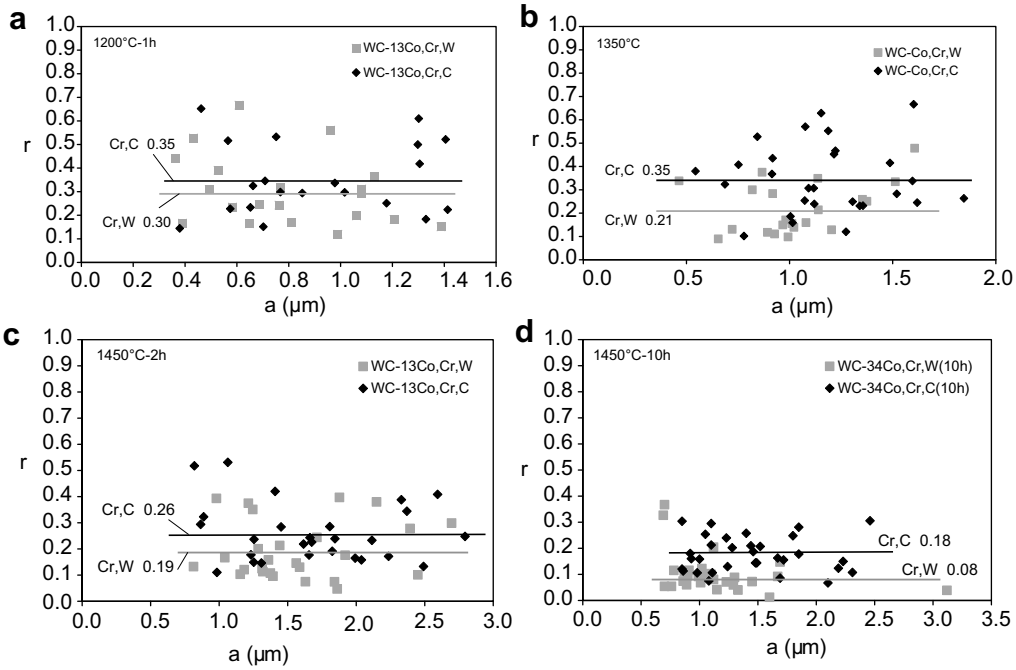

Fig. 5. *r* values versus the grain size recorded after heating at (a) 1200 °C, (b) 1350 °C and (c) 1450 °C for 2 h in WC–13Co, Cr, C and WC–13Co, Cr, W and (d) after 10 h at 1450 °C in WC–34Co, Cr, C and WC–34Co, Cr, W.

detected between the matrix and larger grains in the alloys. These results feature more triangular grains in the W rich alloy (Fig. 5c).

In the alloys containing a larger amount of Co the *r* values are smaller and less scattered (Fig. 4c, d). The mean *r* value is equal to 0.18 ± 0.02 in WC–34Co, Cr, C and to 0.08 ± 0.01 in WC–34Co, Cr, W (Fig. 5d). The whole results point out a smaller truncation factor all along the sintering process for the W rich alloy doped with Cr.

3.3. Study of the WC grain elongation in the Cr doped alloys

After heating for 1 h at 1200 °C, WC grains show smooth basal facets whatever the C content (Fig. 6a, b). The distribution of *k* values is given for both alloys as a function of the grain size. This size is defined as the diameter of a sphere with the same volume as the studied grain. A large scattering is observed whatever the size of the particles (Fig. 7a). The elongation factors are rather close in both alloys regarding the large mean deviation values. The *k* factor is equal to 0.89 ± 0.10 in WC–13Co, Cr, C and to 0.98 ± 0.12 in WC–13Co, Cr, W (Table 3).

When the temperature increases to 1350 °C a larger scattering is observed for the smallest grains. It can be related to the measurement error as discussed in §2.2. After a limit size the values are less dispersed. Only the *k* values measured for the largest grains are considered. Compared to 1200 °C the *k* factors at 1350 °C are nearly unchanged, a value of 0.98 ± 0.11 is recorded in WC–13Co, Cr, C and 0.95 ± 0.12 in WC,13Co, Cr, W (Fig. 7b).

After sintering for 2 h at 1450 °C, the scattering and the elongation decrease in both alloys. *k* attains 0.72 ± 0.06 in WC–13Co, Cr, C and 0.70 ± 0.10 in WC–13Co, Cr, W (Fig. 7c). In the alloys containing a larger amount of Co that were sintered for 10 h at 1450 °C, the elongation is nearly unchanged and no significant difference between the alloys is observed (Fig. 6c, d). The *k* factor is equal to 0.74 ± 0.04 in WC–34Co, Cr, C (10 h) and 0.69 ± 0.07 in WC–34Co, Cr, W(10 h) (Fig. 7d). These results show that the addition of Cr leads to nearly similar *k* factors whatever the C potential.

4. Discussion: effect of Cr addition on the WC grain shape

The evolution of the truncation factors along the sintering stage in undoped alloys was studied in [15]. The results are summarized on Fig. 8 and compared to those of the Cr doped alloys. Nearly no effect of the Cr addition is recorded at 1200 °C and 1350 °C in the C rich and W rich alloys. The addition of Cr significantly decreases the *r* factor after 2 h at 1450 °C in WC–13Co, W alloy and in WC–34Co, W after 10 h at 1450 °C. The study of the grain size evolution in WC–Co alloys as a function of temperature and time shows that grain growth is limited in the WC–34Co, W and very limited in WC–34Co, Cr, W [6]. The shape of WC grains is therefore consid-

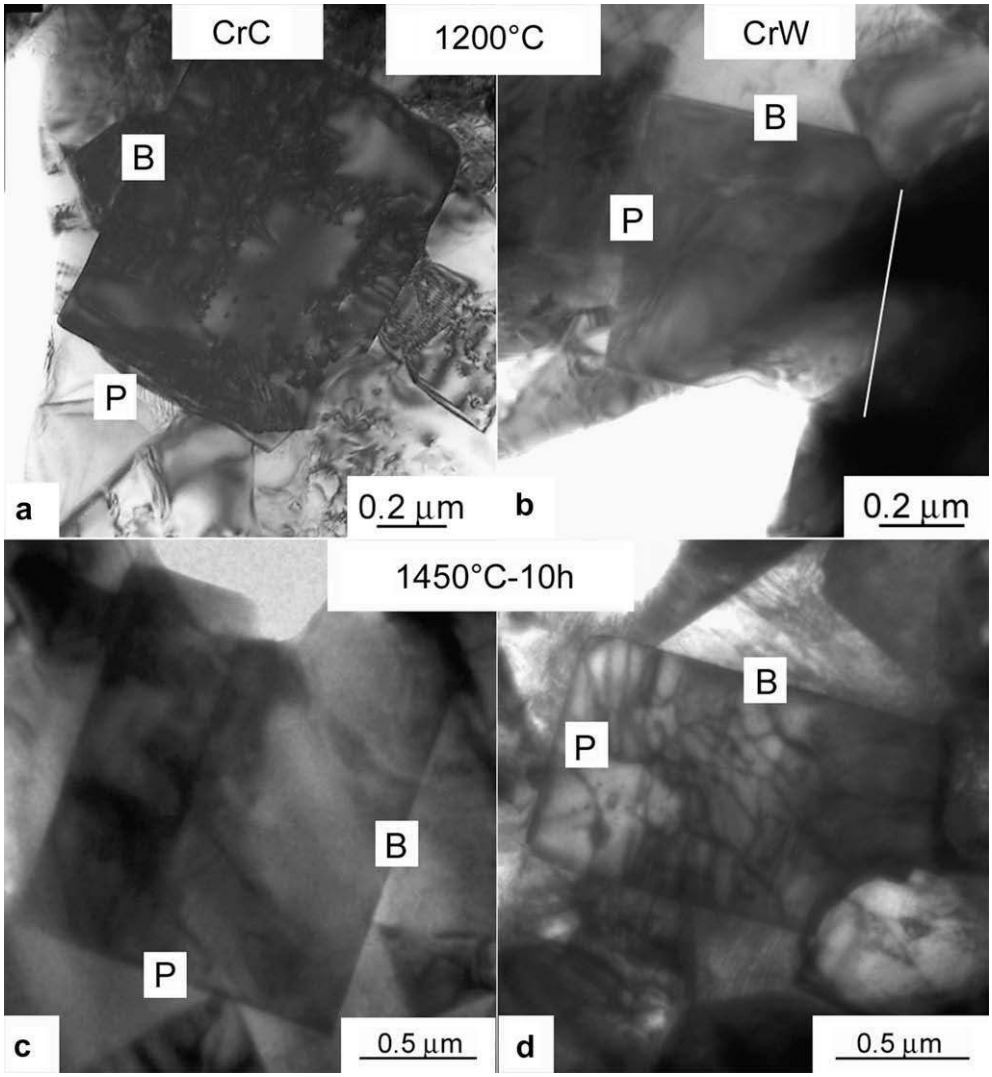

Fig. 6. TEM images of the WC grains viewed along the [11–20] direction in the alloys sintered at 1200 °C (a) WC–13Co, Cr, C with $k = 0.80$ and (b) WC–13Co, Cr, W with $k = 1.08$, and in the alloys sintered for 10 h at 1450 °C (c) WC–34Co, C, Cr (10 h) with $k = 0.81$ (d) WC–34Co, W, Cr with $k = 0.61$. The letters B and P indicate the basal and prismatic facets of the WC grains.

ered close to the equilibrium in these alloys. The shape change would be related to the effect of Cr on the interface energetics of the system. The observations show that the WC grains are more triangular in the Cr doped alloy. The addition of Cr would therefore increase the difference in energy between the two types of prismatic facets in the W rich alloys.

In the C rich alloys, the addition of Cr slightly decreases the r factor after 2 h at 1450 °C and has nearly no effect after 10 h at 1450 °C in the alloy containing a large amount of Co. In the C rich undoped alloys, the WC grain shape alloys is likely influenced by grain growth [15,21]. The addition of Cr has a double effect in these alloys: it limits grain growth and likely modifies the interface energetics. The comparison of the intercept distributions of WC–34Co, Cr, C and WC–34Co, Cr, W and of the related mean intercept values equal to 0.62 µm and 0.53 µm respectively shows that grain growth is also limited in WC–34Co, Cr, C. The shape is likely close to the equilibrium in this alloy. The comparison of WC–34Co, Cr, C and WC–34Co, Cr, W indicates that an excess of C decreases the interface energy anisotropy between the prismatic facets in Cr doped alloys.

The elongation factors in Cr doped and undoped alloys [15] are shown in Fig. 9. The addition of Cr leads to a larger k factor at 1200 °C and 1350 °C in both the C rich and W rich alloys. Then in the C rich alloy, the addition of Cr significantly increases the k factor for the treatments at 1450 °C. In the W rich alloy, the k factor is slightly increased after 2 h at 1450 °C and slightly decreased in WC–34Co, Cr, W (10 h). Similar values are found for the k factors whatever the C content of the Cr doped alloys after 10 h at 1450 °C. The addition of Cr significantly decreases the elongation difference between the alloys sintered at 1450 °C.

The effect of Cr at 1450 °C on the WC grain shape was proposed to result from a Cr segregation at the WC/Co interfaces [22] leading to the formation of a thin (Cr, W)C film in the interfaces at cooling [20].

Microstructural investigations were conducted to study the origin of the effect of Cr already at 1200 °C. Observations were performed at the nanoscale on the WC/Co interfaces. TEM/EDS analyses were carried out in the WC–13Co, Cr, C and WC–13Co, Cr, W alloys. This method does not provide precise compositions of the studied areas but permits to compare the Cr/Co ratios when passing across an interface. The WC grains were oriented along a direction close to $\langle 1\,1\,-2\,0 \rangle$ in order to put the habit planes parallel to the electron beam. The Cr/Co ratios were measured in Co, at the level of WC/Co interfaces and in WC (Fig. 10).

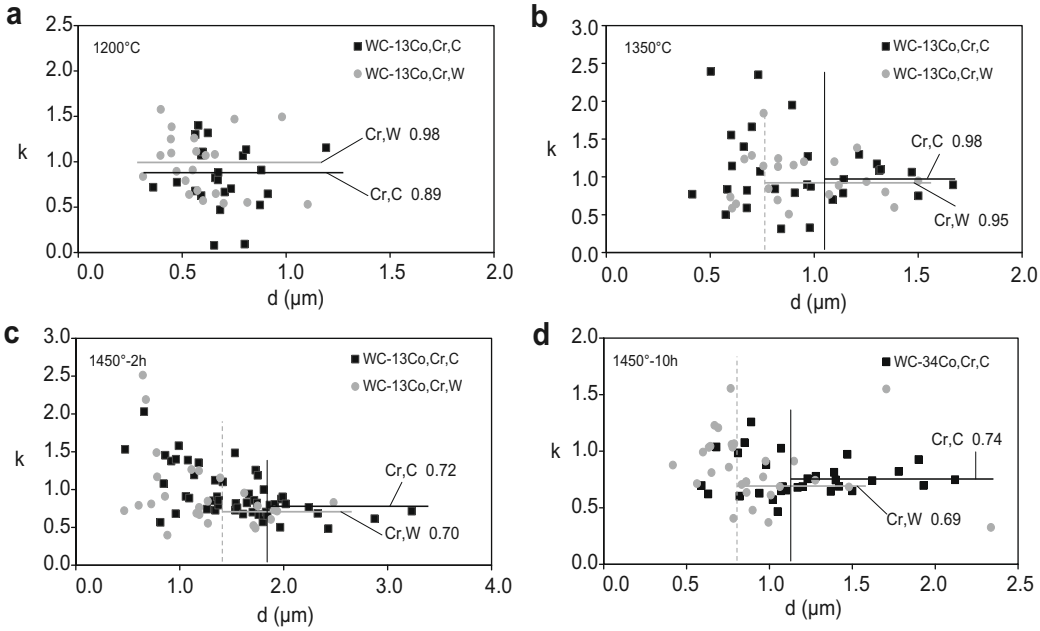

Fig. 7. *k* values versus the grain size recorded after heating at (a) 1200 °C, (b) 1350 °C and (c) 1450 °C for 2 h in WC–13Co, Cr, C and WC–13Co, Cr, W and (d) after 10 h at 1450 °C in WC–34Co, Cr, C and WC–34Co, Cr, W.

Table 3
Mean elongation values *r*, standard deviation of the distribution σ, number of measurements n and reliable interval values recorded for the Cr doped C rich and W rich alloys

	Elongation factor							
	C rich				W rich			
	k	σ	n	$1.7\sigma/\sqrt{n}$	k	σ	n	$1.7\sigma/\sqrt{n}$
1200 °C–1 h	0.89	0.27	21	0.10	0.98	0.33	22	0.12
1350 °C	0.98	0.2	10	0.11	0.95	0.27	15	0.12
1450 °C–2 h	0.72	0.13	13	0.06	0.7	0.16	8	0.1
1450 °C–10 h (34Co)	0.74	0.1	16	0.04	0.69	0.15	13	0.07

Only the data for the largest grains are used for the determination of the *k* factor.

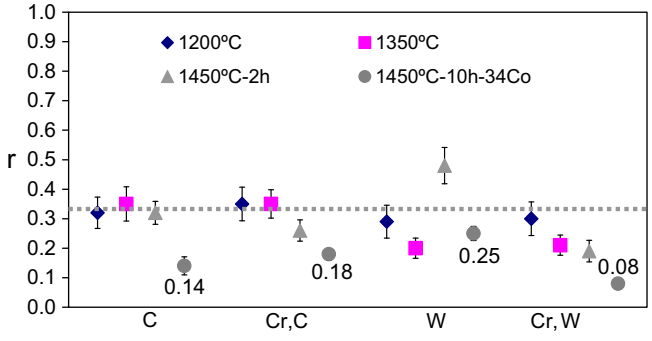

Fig. 8. Summary of the *r* values recorded in the undoped and Cr doped alloys. The dotted line corresponds to the mean *r* value of the undoped alloys at 1200 °C.

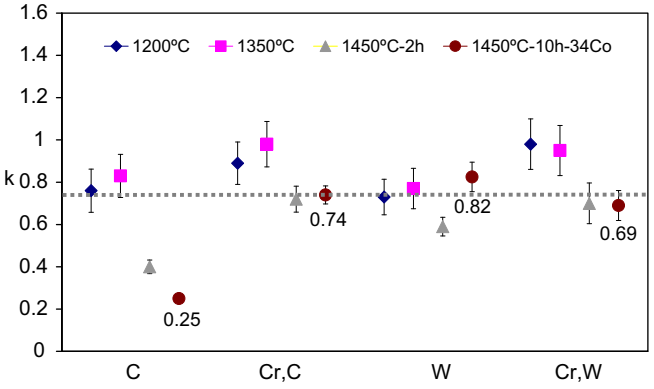

Fig. 9. Summary of the *k* values recorded in the undoped and Cr doped alloys. The dotted line corresponds to the mean value of the undoped alloys at 1200 °C.

No Cr was detected in WC grains as expected from the very low solubility of Cr in WC [23]. The C rate was not analysed. A Cr content of about 4–5 at% was found in the binder close to the starting doping in both alloys. The W level was equal to about 3 at% in WC–13Co, Cr, C and 7 at% in WC–13Co, Cr, W. These values are not quantitative, they agree with the W increase expected in the W rich alloy. An increase of the Cr/Co ratio was found for all studied interfaces. This increase reveals the Cr enrichment of the prismatic and basal interfaces in both types of alloys (Table 4). These results are similar to the investigations performed in a C rich WC–Co alloy sintered at 1200 °C and prepared from Cr doped WC powder [24]. HRTEM images of the WC/Co interfaces were also taken in the WC–13Co, Cr, C alloy (Fig. 11). They show the presence of a very thin layer that fits with the cubic (Cr, W)C compound

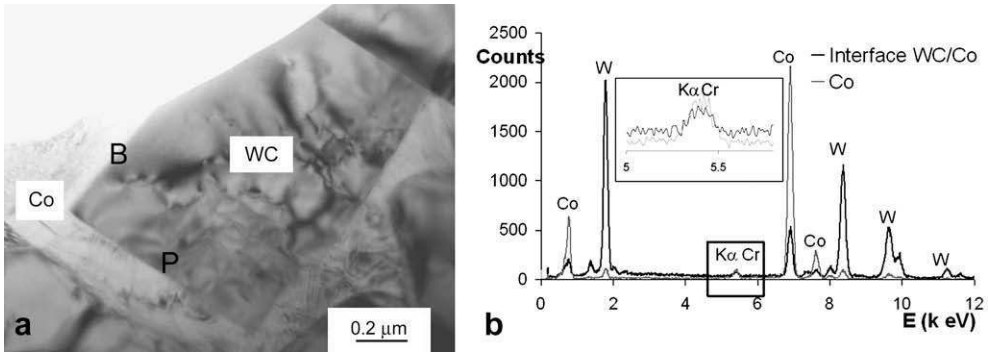

Fig. 10. (a) TEM image of the analysed area in WC–13Co, Cr, C sintered at 1200 °C. The observation direction of the WC grain is close to ⟨11 − 20⟩ (b) Example of EDS spectra of the Co binder and of the prismatic WC/Co interface called *P*.

Table 4
Typical EDS composition (at%) measured in Co binder and at basal and prismatic WC/Co interfaces in WC–13Co, Cr, C sintered at 1200 °C

	Co	W	Cr	Cr/Co
Basal plane				
WC grain	15.2	84.8	0	
Co binder	91.2	4.3	4.5	4.9
Interface	52.3	44.0	3.7	7.1
Prismatic plane				
WC grain	15.2	84.8	0	
Co binder	93.5	1.4	5.1	5.4
Interface	52.6	41.3	6.1	11.5

Due to the size of the beam (∼10 nm) the interface analysis comprises a part of the Co binder and of the WC grain. The analyses correspond to the area shown in Fig. 10 The large amount of Co recorded in the WC grain as well as the variation of the W content for Co close to the prismatic or basal planes are likely due to a deposition of Co and W atoms on the surface of the specimen during the ion beam thinning.

pointed out in the alloys sintered at 1450 °C. This layer orientates differently according to the habit plane of WC as already observed in [20]:$\{0001\}_{WC}$ // $\{111\}_{(Cr,\,W)C}$ with $\langle 11{-}20\rangle_{WC}$ // $\langle -110\rangle_{(Cr,\,W)C}$ $\{1{-}100\}_{WC}$ // $\{001\}_{(Cr,\,W)C}$ with $\langle 11-20\rangle_{WC}$ // $\langle -110\rangle_{(Cr,\,W)C}$

These orientation relationships lead to a very good matching between the two crystal lattices at the interface. Assuming a lattice parameter a = 0.41 nm for the (Cr, W)C compound [20], the misfit values are 0.2% in the basal plane and less than 2.2% in the prismatic plane.

The presence of this thin layer is in agreement with the EDS analyses. The temperature of liquid formation was determined to be 1220 °C in this alloy. Since the thermal treatment was carried out at 1200 °C, and due to local fluctuations in composition, it is not possible to be sure that the liquid has not formed in the alloy at this stage. However in the WC–13Co, Cr, W, the liquid formation occurs at 1330 °C and the Cr enrichment of the interfaces is detected by EDS analyses. These results likely indicate a segregation of Cr already at 1200 °C. They suggest an effect of Cr on the interface energies already at the solid state in agreement with the increase of the elongation factor recorded at this temperature in the Cr doped alloys.

The interface energy ratios can be deduced from the shape factors determined in the alloys where the WC grain morphology is assumed to be close to the equilibrium. The values obtained in WC–34Co, C are indicated but are likely influenced by the grain growth process (Table 5). The results show that the addition of Cr in the W rich alloy results in an increase of the anisotropy between the prismatic planes while the anisotropy is smaller in the C rich alloy. The interface energy ratio between the basal and the prismatic facets is slightly decreased by the Cr addition in the W rich alloy. It is noticeable that the ratio between the energy of the basal and the prismatic facets is the same in the W and C rich alloys containing Cr. Moreover the ratio is close to 1 what indicates energy values in the same range for the basal and the longest prismatic facets in the Cr doped alloys. This result agrees with the rounding of the interfaces observed in these alloys [9].

Table 5
Ratios of the interface energies deduced from the shape factors in the assumption of an equilibrium shape

Alloy	r	$\gamma^{Plong}/\gamma^{Pshort}$	k	$\gamma^{B}/\gamma^{Plong}$
WC–34Co, C	0.14	0.60	0.25	0.33
WC–34Co, W	0.25	0.67	0.82	1.03
WC–34Co, Cr, C	0.18	0.62	0.74	0.96
WC–34Co, Cr, W	0.08	0.56	0.69	0.96

The values associated with the WC–34Co, C alloy are likely not at the equilibrium.

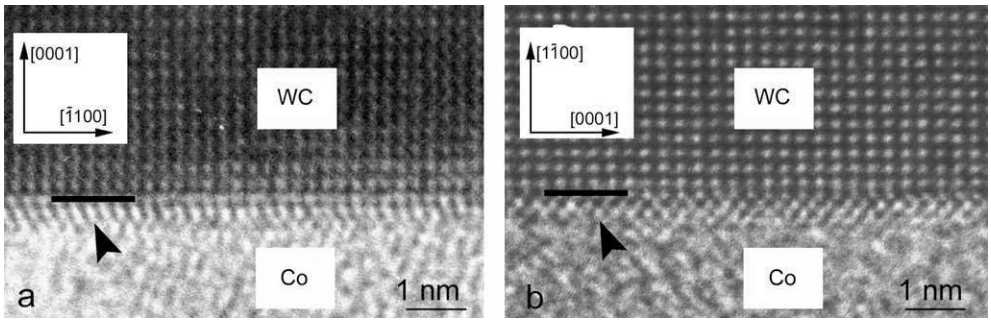

Fig. 11. HRTEM images of WC/Co interfaces viewed along the ⟨11 − 20⟩ direction of WC in WC–13Co, Cr, C sintered for 1 h at 1200 °C. The arrows indicate a thin crystalline layer about 1 nm in thickness at the interface between WC and Co (a) at the basal and (b) at the prismatic facets of the WC grains.

5. Conclusion

In this work, an experimental approach is used to quantify the WC grain shape during the sintering of Cr doped WC–Co alloys as a function of the C and Co content. Main results are as follows:

- An effect of the Cr addition is already recorded at 1200 °C ie at the solid state. For this temperature microstructural investigations detect a Cr enrichment at the WC–Co interfaces that is likely associated with a change in interface energetics.
- During liquid phase sintering, the WC grain morphology evolves as a function of the composition.
  - o The grains are a little more triangular on the W rich side than on the C rich side in the Cr doped alloys. They become more triangular in the alloys sintered for the longest time and containing a larger content of Co. Compared to the undoped alloys, the strongest effect occurs in the W rich alloys where the *r* factor significantly decreases.
  - o On the other hand, the elongation factors become very similar in both types of Cr doped alloys and no change is observed after a longer sintering time. It is noticeable that the addition of Cr seems to lead to rather similar energies for the basal and the longest prismatic facets whatever the C potential. Compared to the undoped alloys, the *k* factor significantly increases in the C rich alloys.

Further experimental investigations at the atom scale would be useful to provide information on the effect of Cr on the WC/Co interfaces. Especially, the atomic change of the interface structure should be studied. These data could be used to model the interfaces in Cr doped alloys and calculate the energies of the facets.

Acknowledgements

This work was supported financially by Sandvik Hard Materials and by the french national association for technical research (ANRT). The authors are grateful to Dr C. H. Allibert, INPGrenoble, and E. Pauty, Sandvik Hard Materials, for fruitful discussion and advice.

References

[1] Exner HE. Physical and chemical nature of cemented carbides. Int Met Rev 1979;4:149–73.
[2] Schubert WD, Boch A, Lux B. General aspects and limits of conventional ultrafine WC powder manufacture and hard metal production. Int J Refract Met Hard Mater 1995;13:281–96.
[3] Allibert CH. Sintering features of cemented carbides WC–Co processed from fine powders. Int J Refract Met Hard Mater 2001;19:53–61.
[4] Hayashi K, Fuke Y, Suzuki H. Effects of addition carbides on the grain size of WC–Co alloy. J Jap Soc Powder Met 1972;19:67–71.
[5] Wang Y, Heusch M, Lay S, Allibert CH. Microstructure evolution in the cemented carbides WC–Co I. Effect of the C/W ratio on the morphology and defects of the WC grains. Phys Status Solidi A 2002;193:271–83.
[6] Chabretou V, Allibert CH, Missiaen JM. Quantitative analysis of the effect of the binder phase composition on the grain growth in WC–Co sintered materials. J Mater Sci 2003;38:2581–90.
[7] Kim S, Han SH, Park JK, Kim HE. Variation of WC grain shape with carbon content in the WC–Co alloys during liquid phase sintering. Scripta Mater 2003;48:635–9.
[8] Kim CS, Massa TR, Rohrer GS. Interface character distributions in WC–Co composites. J Am Soc 2008;91:996–1001.
[9] Wang Y, Pauty E, Lay S, Allibert CH. Microstructure evolution in the cemented carbides WC–Co II. Cumulated effects of Cr additions and of the C/W ratio on the crystal features of the WC grains. Phys Status Solidi A 2002;193:284–93.
[10] Lee HR, Kim DJ, Hwang NM, Kim DY. Role of vanadium carbide additive during sintering of WC–Co: mechanism of grain growth inhibition. J Am Ceram Soc 2003;86:152–4.
[11] Shatov AV, Firstov SA, Shatova IV. The shape of WC crystals in cemented carbides. Mater Sci Eng A 1998;242:7–14.
[12] Warren R. Determination of the interfacial energy ratio in two-phase systems by measurement of interphase contact. Metallography 1976;9:183–91.
[13] Christensen M, Dudiy S, Wahnström G. First-principles simulations of metal-ceramic interface adhesion: Co/WC versus Co/TiC. Phys Rev B 2002;65: 045408-1–8-9.
[14] Christensen M, Wahnström G, Lay S, Allibert CH. Morphology of WC grains in WC–Co alloys: theoretical determination of WC grain shape. Acta mater 2007;55:1515–21.
[15] Delanoë A, Lay S. Evolution of the WC grain shape in WC–Co alloys during sintering: effect of C content. Int J Refract Met Hard Mater 2008. doi:10.1016/j.ijrmhm.2008.06.001.
[16] Lavergne O, Robaut F, Hodaj F, Allibert CH. Mechanism of solid-state dissolution of WC in Co-based solutions. Acta Mater 2002;50:1683–92.
[17] Lavergne O, Allibert CH. Dissolution mechanism of tungsten carbide in cobalt-based liquids. High Temp High Press 1999;31:347–55.
[18] Delanoë A, Missiaen JM, Allibert CH, Lay S, Pauty E. Effect of the C potential and of Cr doping on the densification of alloys WC–Co. In : Kneringer G, Rodhammer P, Wilner H, editors. Powder Metallurgical High Performance Materials, Plansee Holding AG, Reutte, Tyrol, Austria, Proceedings of the 16th Intern Plansee Seminar, vol 2; 2005. p. 642–52.
[19] Akesson L. Dissertation, Stockholm, Sweden: Royal Institute of Technology; 1982.
[20] Delanoë A, Bacia M, Pauty E, Lay S, Allibert C. H. Cr-rich layer at the WC/Co interface in Cr-doped WC–Co cermets: segregation or metastable carbide? J Cryst Growth 2004;270:219–27.
[21] Lay S, Allibert CH, Christensen M, Wahnström G. Morphology of WC grains in WC–Co alloys. Mater Sci Eng A 2008;486:253–61.
[22] Yamamoto T, Ikuhara Y, Watanabe T, Samuka T, Taniuchi Y, Okada K, et al. High resolution microscopy study in Cr3C2-doped WC–Co. J Mater Sci 2001;36:3885–90.
[23] Henjered A, Hellsing M, Andren H-O, Norden H. Quantitative microanalysis of carbide/carbide interfaces in WC–Co base cemented carbides. Mater Sci Tech 1986;2:847–55.
[24] Elfwing M, Norgren S. Study of solid-state sintered fine-grained cemented carbides. Int J Refract Met Hard Mater 2005;23:242–8.